Vol 15 No 8, August 2006
1009-1963/2006/15(08)/1903-06

Chinese Physics

© 2006 Chin. Phys. Soc.
and IOP Publishing Ltd

Rapid Communication

High-T_c planar SQUID gradiometer for eddy current non-destructive evaluation*

Zhang Ming-Jian(张鸣剑)[a], Lang Pei-Lin(郎佩琳)[a)b)], Peng Zhi-Hui(彭智慧)[a)], Chen Ying-Fei(陈莺飞)[a)], Chen Ke(陈　珂)[a)], and Zheng Dong-Ning(郑东宁)[a)†]

[a)] *National Laboratory for Superconductivity, Institute of Physics, and National Laboratory for Condensed Matter Physics, Chinese Academy of Sciences, Beijing* 100080, *China*

[b)] *Department of Physics, Tsinghua University, Beijing* 100084, *China*

(Received 9 February 2006; revised manuscript received 3 April 2006)

This paper reports the fabrication and test of a high-T_c SQUID planar gradiometer which is patterned from YBCO thin film deposited on a $SrTiO_3$ bicrystal substrate. The measurement of noise spectrum at 77K shows that the white noise at 200 Hz is about $1\times10^{-4}\,\Phi_0/\sqrt{\text{Hz}}$. The minimal magnetic gradient is measured and the results suggest that the minimal magnetic gradient is 94 pT/m. The planar gradiometer is used in non-destructive evaluation (NDE) experiments to detect the artifacts in conducting aluminium plates by performing eddy current testing in an unshielded environment. The effect of the exciting coil dimension on the NDE results is investigated. By mapping out the induced field distribution, flaws about 10mm below the plate surface can be clearly identified.

Keywords: SQUID, planar gradiometer, NDE
PACC: 7360K, 0670E

1. Introduction

Superconducting quantum interference devices (SQUIDs) are the most sensitive sensors in detecting magnetic flux and have been widely used in many noninvasive applications.[1] The very high magnetic field sensitivity down to 1 $\text{fT/Hz}^{1/2}$, wide bandwidth from DC to hundreds of kHz and large dynamic range of over 100dB possessed by SQUIDs make them attractive as sensors in non-destructive evaluation (NDE),[2−6] magnetocardiography (MCG),[7−9] geophysical measurement and other applications. In many practical applications, environmental noise can suppress the usable dynamic range of SQUID devices and hence deteriorate the performance of the system. To solve this problem, one may utilize a SQUID gradiometer such as the planar gradiometer or electronic gradiometer.[10,11] Up to now, a wide variety of different designs of first- and second-order high-T_c SQUID gradiometers have been demonstrated.[12−14] A first-order planar gradiometer can be made from a single layer of high-T_c thin film with two symmetric pickup loops directly coupled to a SQUID. A number of researches have experimentally demonstrated sufficient sensitivities of magnetic field measurements using high-T_c gradiometers for NDE, and even for MCG signal in unshielded environments.[15−17] In this paper, we report the fabrication and characterization of a YBCO first-order planar gradiometer and its application in NDE. Using this gradiometer, we have measured the field distribution due to induced eddy currents in NDE measurements. The results show that flaws 10mm below the surface in conducting aluminium plates and other structures can be clearly identified. Additionally, the effect of excitation coil on the result is also discussed.

2. The design and fabrication of first-order planar gradiometer

As mentioned above, in order to make SQUID measurements more stable and measure very weak magnetic signal such as MCG signals in a magneti-

*Project supported by Ministry of Science and Technology of China (Grant Nos 2006CB601007 and 2002AA306412), National Nature Science Foundation of China (Grant No 10221002) and Chinese Academy of Sciences and National Center for Nanoscience and Technology, China.
†Corresponding author. E-mail: dzheng@ssc.iphy.ac.cn

cally unshielded environment, gradiometers are commonly used. For conventional low-T_c devices, a gradient pickup coil can be made by using thin superconducting metal wires and coupled to a SQUID. For high-T_c oxide superconductors, however, there is no wire suitable for making gradient coils at present, and hence the use of planar gradiometers is the choice of an alternative approach.

We have designed a first-order planar gradiometer on bicrystal substrate. Figure 1(a) shows the scheme of the gradiometer. Two pickup loops (1 and 2) are the flux antennae that have the loop areas of A_1, A_2 and the inductances of L_1, L_2 respectively. The two loops are connected to each other by a common central stripe (3). The dc-SQUID (4) is directly coupled to the central stripe line. In a symmetrical situation, we assume that $L_1 = L_2 = L_a$ and $A_1 = A_2 = A_a$. It is obvious that the flux (Φ) through the SQUID hole is proportional to the field gradient of the two pickup loops as shown in the following formula:

$$\Phi = bA_a(L_M/L_a) \cdot (\partial B/\partial x) = bA_{eff} \cdot \partial B/\partial x, \quad (1)$$

where b is the baseline between the two antennae, L_M is the mutual inductance between the antennae and the SQUID hole, and A_{eff} is the effective area of the gradiometer. For the purpose of making a SQUID of such design on a 10 mm×10 mm STO bicrystal, we designed a layout as shown in Fig.1(a). The outer dimension of the gradiometer is 8 mm×8 mm. The line width of the antennae is 1000 μm, the area of central SQUID hole is 4 μm×90 μm, and the junction width is 4 μm, as shown in Fig.1(b). The baseline for this gradiometer, taken as the distance between the geometric centres of the right-hand and left-hand antenna, is about 6 mm.

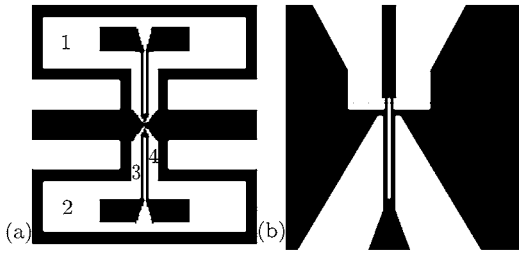


Fig.1. Layout of (a) the complete gradiometer sensor and (b) the DC SQUID at the inner part of the sensor (the dashed line indicates the grain boundary).

The gradiometer we fabricated was based on YBCO thin films. The substrate used was 10 mm×10 mm×0.5 mm (100) $SrTiO_3$ bicrystal with a symmetric misorientation angle at the grain boundary of 24°. A thin YBCO layer was grown in situ on the substrate epitaxially by pulsed laser deposition (PLD) technique. The deposition was carried out at 40 Pa oxygen pressure and at a substrate temperature about 800°C. It was confirmed by x-ray diffraction that the film was of single phase and grown epitaxially with the c-axis perpendicular to the surface of the film. After the deposition, a thin layer of Au (∼80nm) was sputtered on electric pad areas. The superconducting transition temperature of the film, as determined in transport measurement, is above 88K. The gradiometer was then patterned with the junctions at the grain boundary by using standard lithography and ion milling method. In order to reduce the heating effect during ion-milling which could degrade the superconducting properties around the junction area. The ion-current used was kept to a relatively low level.

3. Characterization of the gradiometer

The characterization of the magnetometer was carried out at 77 K by mounting the sample in a measurement probe which was immersed into a liquid nitrogen dewar. Figure 2 shows the temperature dependence of the resistance and the I–V characteristics measured at 77 K in a μ-metal shielded space. The data of the I–V curve show that the device does not exhibit zero resistance at 77 K. It appears that there is a resistance which is in series with the junctions. The value of the resistance may be estimated by taking the slope near the zero voltage in Fig.2(b). We note that this value is the same as the residual resistance value in the inset of Fig.2(a). The I–V curve after the subtraction of the residual resistance is shown in the inset of Fig.2(b). Clearly, the device exhibits a RSJ-like I–V curve with a critical current (I_c) about 25 μA and a normal resistance (R_n) about 1.4Ω. The product of I_cR_n is about 35 μV. The voltage response to external magnetic flux is illustrated in Fig.3. The transfer coefficient of the modulation system is about 20 $\mu V/\Phi_0$.

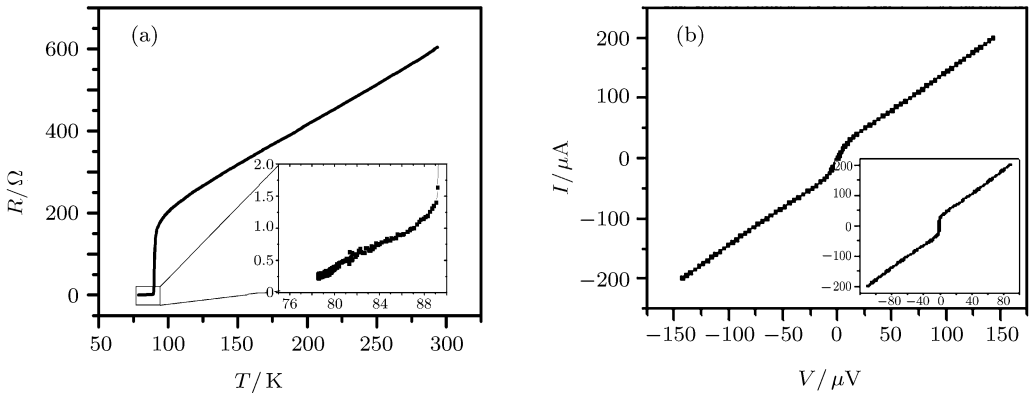


Fig.2. (a) The resistance versus temperature characteristics of the devices. (b) Current versus voltage characteristics at 77 K of the central SQUID. The inset shows the data after subtraction, the value of the resistance is estimated by taking the slope near the zero voltage in Fig.2 (b).

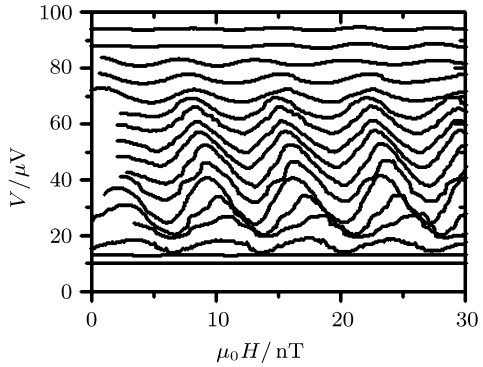


Fig.3. The modulation curves of the same gradiometer at different bias. The I_b is 5μA on the bottom line. For the other lines I_b is increased by 5μA one by one from the bottom to the top.

The gradiometer worked in a flux-locked loop configuration with a 50 kHz modulation frequency F. The modulation field was supplied by a small coil wound with copper wire attached on the top of the device. After the loop being locked, the output voltage was recorded by a spectrum analyser. Shielding against external interference fields was provided by three layers of μ-metal foil which were wrapped up around the dewar. The flux noise spectrums S_ϕ of the gradiometer is shown in Fig.4(a). As shown, the white noise at 200 Hz is about $1\times10^{-4}\Phi_0/\sqrt{\mathrm{Hz}}$.

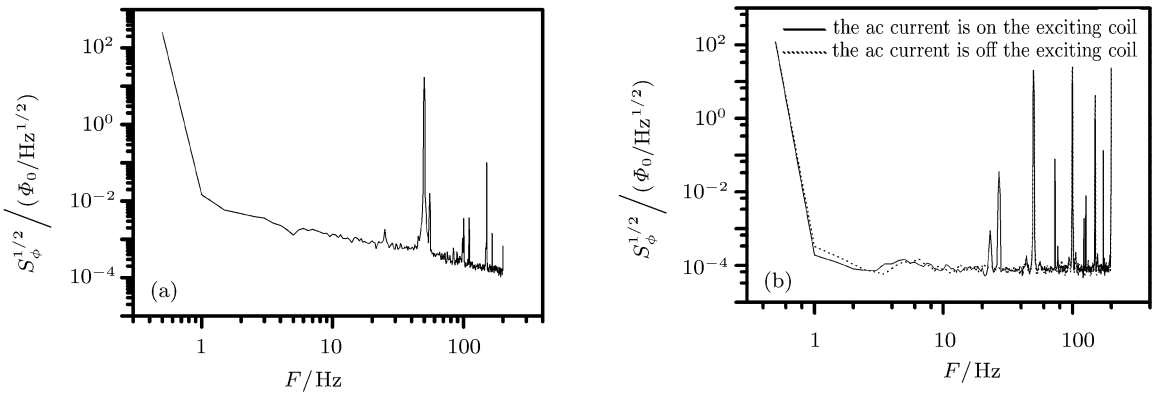


Fig.4. (a) The flux noise spectrum of the gradiometer shielded by three layers of μ-metal foil. (b) The flux noise spectrum of the gradiometer in unshielded environment. The dashed line represents the noise spectrum when the AC current in the exciting coil is switched off while the solid line represents the noise spectrum when the AC current is on the exciting coil which was applied 83Hz and 0.2V alternating voltage.

We have also measured the noise spectrum in an unshielded environment and the results are presented in Fig.4(b). It was performed in a dewar used for NDE experiment. Exciting coil for generating eddy current was mounted outside the dewar and attached on the bottom surface. The dashed line represents the noise spectrum when the AC current in the exciting coil is switched off while the solid line represents the noise spectrum when the AC current is switched on. The AC current was generated by connecting the coil to an alternating voltage source at frequency 83 Hz and amplitude 0.2V. From the Fig.4(b), we can see that two lines are nearly coincident. When we injected the exciting current, there was only added frequency multiplication component of 83Hz in noise spectrum, whereas white noise level was almost identical. In pre-

vious NDE experiments,[2,3] we used a SQUID magnetometer instead of a gradiometer, and found that it was rather difficult to lock in an unshielded environment due to external noise. The above results suggest that the gradiometer can effectively suppress the unwanted noise and work in an unshielded environment.

In order to measure the gradient field sensitively of the gradiometer, we designed an experiment in which a rectangular coil of 10 cm×20 cm was used. We made one side of the coil to approach the gradiometer, and measured the output of the gradiometer. When the coil was passed with a 40 μA current and one side was near to the gradiometer which was 4 cm away from the device, SQUID electronics gave an output signal of 3.2 mV. Because another side of the coil was far away from the gradiometer, so we could consider the impact of the side near the device only. Therefore we could calculate that the magnetic gradient of the coil in the gradiometer was 5nT/m. Considering the transfer coefficient was $20\mu\mathrm{V}/\Phi_0$ and the amplifying factor of SQUID electronics was about 30000, we calculated that the minimal magnetic gradient was about 94pT/m, which could be measured by the gradiometer.

4. Eddy-current NDE using high-T_c gradiometer

Since SQUIDs are extremely sensitive magnetic flux-voltage transformers, they can be used as sensors in the field of eddy current NDE. In some NDE applications, the use of SQUIDs is the best or even the unique method for electromagnetic field measurement. To carry out the NDE investigation by using high-T_c SQUIDs, we have made an experimental testing setup that was described in details elsewhere.[2] When a SQUID device was used, the exciting coil was made in a double-D shape in order to minimize the effect on the SQUID device. Here, we used a SQUID gradiometer, and hence the exciting coil was a round coil. Before starting to perform eddy current NDE measurement, a small AC current was applied to the exciting coil. By moving the exciting coil slowly around the device so that the output of the gradiometer is minimum.

Firstly we carried out measurements by using exciting coils with different dimensions to optimize the spatial resolution. We piled up six 180 mm×180 mm×2 mm aluminium plates on the sample stage which could move horizontally in x and y directions. In the middle of them, the third plate from top was made up of two 90 mm×180 mm×2 mm plates. The top surface of the plates was about 11 mm away from the bottom of the gradiometer. During measurements, a 2 V/113 Hz AC voltage from a lock-in amplifier was applied to the round coil, which produced eddy current signals in aluminium plates. The gradiometer detected the eddy current signals, which were collected through the lock-in amplifier and recorded by a computer. Figure 5 shows the results for three coils with different dimension of 4mm, 22mm, 30mm, and the number of turns is 10, 18, 10 respectively.

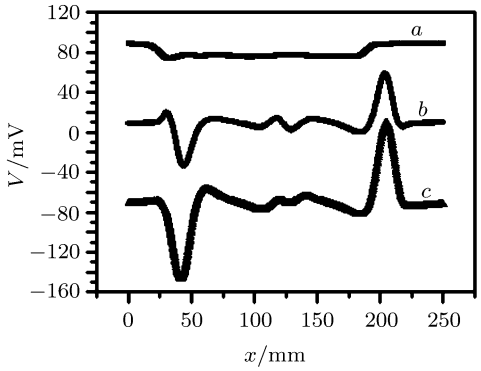


Fig.5. The scanning curves obtained by using different exciting coils. Curve *a* The diameter of exciting coil is 4mm. Curve *b* the diameter of exciting coil is 22mm. Curve *c* the diameter of exciting coil is 30mm. For clarity, each curve is displaced vertically by 80mV.

As for the large exciting coil, the magnetic field in the interesting area could be regarded approximately to be uniform, therefore the eddy current was also uniform except for the flaw region in the aluminium. When one of the pick-up loops of the gradiometer passed on the flaw, there would be a positive (or negative) voltage, but when another pick-up loop passed, there would be a voltage signal of opposite sign, as shown in curve *b* or curve *c*. For the small exciting coil, we suggest that the eddy current signal was local, and the magnetic field caused by the eddy current could be considered as a point source. When the gradiometer moved on the flaw, the eddy currents from the two sides of the flaw could be regarded as two point sources. However, the distance between the two point sources was less than the baseline of the gradiometer, so the change of the magnetic gradient was very small. Curve *a* in Fig.5 shows experimental results for the small exciting coil. From the curve *b* and the curve *c*, we can see that the signal using the medium-coil is clearer than that using the large-coil. However, the position resolution is similar for the two coils. The stronger signal using

the medium coil is probably caused by the stronger field, and subsequently larger eddy current produced by medium coil that has 18 turns as compared to the 10 turns of the large coil. From the above results we believe that the spatial resolution is primarily decided by the baseline. As for the exciting coil, it is better to choose a coil of dimension larger than the baseline of the gradiometer in order to eliminate the influence caused by the shape of the coil. On the other hand, the coil dimension should not be too large so that the strength of the magnetic field at the centre is not too small.

Secondly, we investigated the effect of the flaw depth by placing the aluminium plate with a flaw in different layers. We put the sample on the moving stage and adjusted the flaw parallel to the central slit of the driving coil. During measurement, the medium-coil was adopted and the voltage of the driving coil was the same as that in the anterior experiment. The measurement results are shown in Fig.6, in which z represents the layer at which the flaw plate was placed. We can see that besides the edge effects, there is clearly a slit effect for the samples. Figure 6(a) shows the real part of the signal and Fig.6(b) shows the imaginary part of the signal. The thickness of each aluminium plate is 2 mm, thus flaws about 10mm below the top plate surface can be clearly identified.

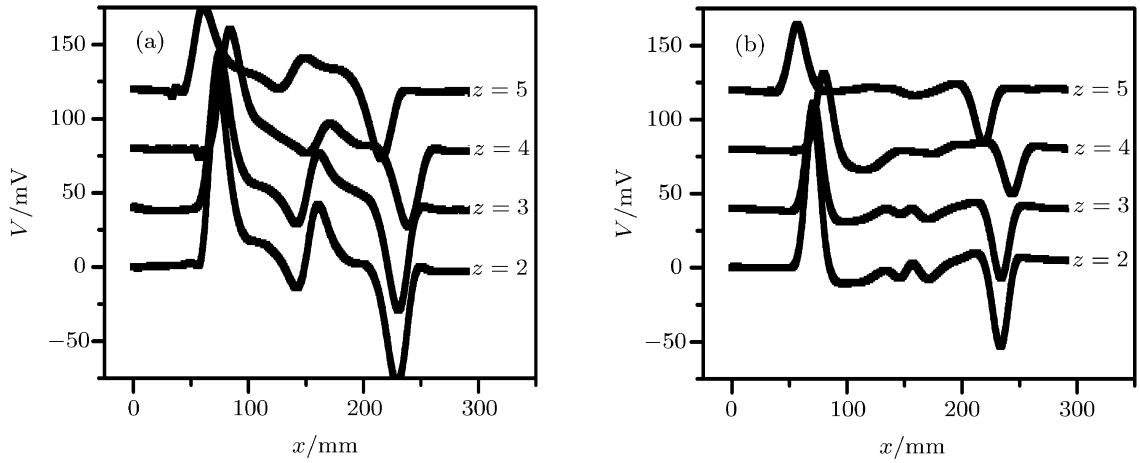


Fig.6. The scanning curves obtained for the flaw of different depths. (a) The real part of the signal. (b) The imaginary part of the signal. z shows the position of the flaw. For clarity, each curve is displaced vertically by 20mV.

Finally, we replaced the flaw plate with another one, in this plate an 'E'-like cut was made to construct a known crack. On the top of the flaw plate we put one layer of aluminium plate without crack. To distinguish the shape of the crack, we made the plates move in x and y directions in a zigzag style. The baseline was perpendicular to the three slits in the 'E' like cut. The contour mapping of the amplitudes of the eddy current signals from the measured samples was plotted according to the position. As shown in Fig.7, the three slits can be clearly discerned in the mapping. The distance between the two slits is 10 mm in the sample, thus we know that the spatial resolution of the gradiometer is 10 mm at least.

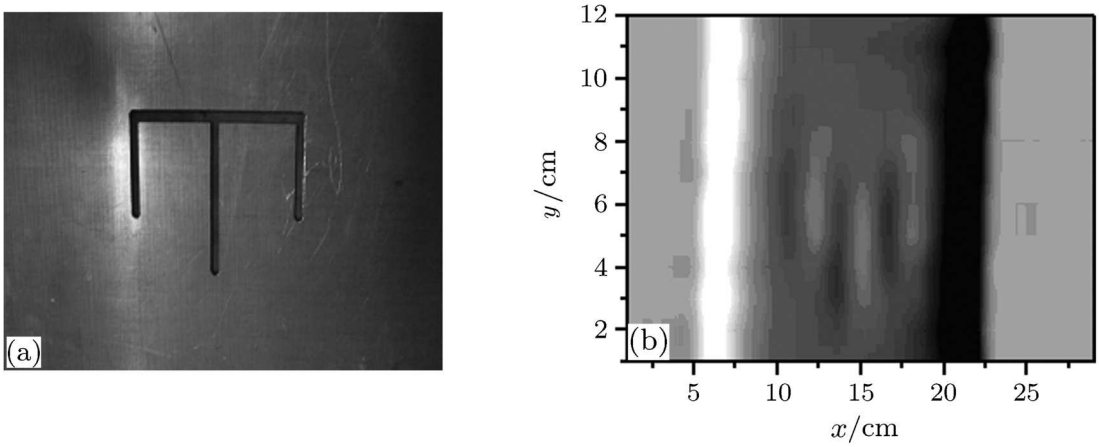


Fig.7. Photograph (a) and NDE contour line graph (b) of an aluminium plate with an artifact structure. The structure shows an 'E' like configuration.

5. Conclusions

In summary, we have fabricated a HTS gradiometer based on YBCO thin films. The gradiometer was made on a $SrTiO_3$ bicrystal substrate and operated at 77K. The response to the field modulation and the noise characteristics has been investigated. We have carried out eddy current NDE measurement by using this gradiometer. The data shows that flaws hiding 10 mm below the surface in conducting aluminium plates can be clearly identified in an unshielded environment. We have also studied the effect of exciting coil dimensions on the results. It appears that an exciting coil with a dimension larger than baseline length could give clear image of cracks.

References

[1] Jenks W G, Sadeghi S S H and Wikswo J P 1997 *J. Phys.* D: *Appl. Phys.* **30** 293

[2] Chen K, Chen L, Yang T, Wang J P, Wu P J, Zheng D N and Zhao Z X 2000 *Physica* C **329** 102

[3] Wang H W, Kong X Y, Ren Y F, Yu H W, Ding H S, Zhao S P, Chen G H, Zhou Y L, Zhang L H, He Y S and Yang Q S 2003 *Chin. Phys.* **13** 19

[4] Carr C, Cochran A, Kuznik J, Mckirdy Mca D and Donaldson G B 1996 *Cryogenics* **36** 691

[5] Travrin Y, Krause H J, Wolf W, Glyantsev V, Schubert J, Zander W and Bousack H 1996 *Cryogenics* **36** 83

[6] Wikswo J P Jr 1995 *IEEE Trans. Appl. Supercond.* **5** 74.

[7] Zhang Y, Tavrin Y, Mück M, Braginski A I, Heiden C, Hampson S, Pantev C and Elbert T 1993 *Brain Topography* **5** 379

[8] Dijorio M S, Yang K Y and Yoshizumi S 1995 *Appl. Phys. Lett.* **67** 1926

[9] Curio G, Drung D, Koch H, M ü ller W, Steinhoff U, Trahms L, Shen Y Q, Vase P and Freltoft T 1996 *Neurosci. Lett.* **206** 204

[10] Schultze V, Stolz R, LJsselsteijn R, Zakosarenko V, Fritzsch L, Thrum F, II'ichev E and Meyer H G 1997 *IEEE Trans. Appl. Supercond.* **7** 3473

[11] Travin Y, Zhang Y, M ü ck M, Braginski A I and Heiden C 1993 *IEEE Trans. Appl. Supercond.* **3** 2477

[12] Kittle A, Kouznetsov K A, McDermott R, Oh K and Clarke J 1998 *Appl. Phys. Lett.* **73** 2197

[13] Lee Soon-Gul, Hwang Yunseok, Nam Byung-Chang, Kim Jin-Tae and Kim In-Seon 1998 *Appl. Phys. Lett.* **73** 2345

[14] Lang P L, Chen K, Zheng D N, Zhang M J, Qi H H and Zhao Z X 2004 *Acta Phys. Sin.* **10** 3530 (in Chinese)

[15] Jeng J T, Horng H E and Yang H C 2002 *Physica* C **368** 105

[16] Kasai N, Suzuki D, Takashima, Koyanagi H and Hatsukade M Y 1999 *IEEE Trans. Appl. Supercond.* **9** 4393

[17] Krause H J and Kreutzbruck M V 2002 *Physica* C **368** 70